# Activated carbon from flash pyrolysis of eucalyptus residue

**Grima-Olmedo C** [a,*], **Ramírez-Gómez Á** [b], **Gómez-Limón D** [a], **Clemente-Jul C** [a]

[a] *Escuela Técnica Superior de Ingenieros de Minas y Energía. Calle Ríos Rosas 23, 28003 Madrid. Universidad Politécnica de Madrid (UPM)*

[b] *Escuela Técnica Superior de Ingeniería y Diseño Industrial. Ronda de Valencia 3, 28012, Madrid. Universidad Politécnica de Madrid (UPM)*

\* Corresponding author.

E-mail address: carlos.grima@upm.es (C. Grima-Olmedo).

## Abstract

Forestry waste (eucalyptus sp) was converted into activated carbon by initial flash pyrolysis followed carbonization and $CO_2$ activation. These residues were obtained from a pilot plant in Spain that produces biofuel, the biochar represented 10–15% in weight. It was observed that the highest activation was achieved at a temperature of 800 °C, the specific surface increased with time but, on the contrary, high loss of matter was observed. At 600 °C, although there was an important increase of the specific surface and the volume of micropores, at this temperature it was observed that the activation time was not an influential parameter. Finally, at 400 °C it was observed that the activation process was not very significant. Assessing the average pore diameter it was found that the lowest value corresponded to the activation temperature of 600 °C, which indicated the development of microporosity. When the activation temperature increases up to 800 °C the pore diameter increased developing mesoporosity.

Keywords: Engineering, Agriculture

## 1. Introduction

Activated carbon is a form of carbon that has been processed to create pores, resulting in an increased surface area. The surface area of activated carbon makes the material suitable for many processes: metal extraction from industrial waste

water [1, 2, 3 and 4], water purification [5, 6], sewage treatment [7, 8], air conditioning filters [9], gas masks manufacturing [10, 11], etc.

Activated carbon can be produced from carbonaceous source materials such as eucalyptus wood [12] and acacia [13, 14], waste wood from old wooden houses and tips in saw-mills [15], lignin (which is a waste emitted from paper mill and that normally is used like fuel) [16], cork oak [17], apricot stone [18], peanut shell [19], rice husks [20], ears of corn [21] or cellulose-based paper impregnated with a petroleum pitch [22].

The process to obtain an activated carbon begins with the pyrolyzation, dehydration and volatilization of the specimen. Therefore, biochar with high carbon content is obtained after elements that are non-carbonaceous such as hydrogen and oxygen are eliminated. The pyrolysis process is performed in the absence of oxygen in order to avoid combustion. The specimen starts to develop an internal porosity, low compared to that developed afterwards during the activation process. Tar substances and carbonaceous residues detached during heating are eliminated during the activation process, opening current pores and developing new ones. The activation can be achieved following a physical [23] or a chemical [24, 25 and 26] procedure.

Physical activation involves carbonization followed by activation of the resulting char in the presence of activating agents. As to the possible physical treatments, the one standing out uses water vapour [27, 28, 29 and 30] or carbon dioxide as activating gas [31, 32], or a mixture of both [33].

Chemical activation is known as a single step method for the preparation of activated carbon in the presence of chemical agents. Chemical activation usually requires lower temperatures and shorter times for activation of the material. It can improve the pore development in the carbon structure because the effect of chemicals. The carbon yields obtained by chemical activation are higher than by physical activation. However, it requires a process after the thermal treatment that recovers the chemical agents, which might restrict its application due to environmental issues [34].

The main characteristic of the activated carbon is that possess a high adsorption capacity, as a result of the high degree of microporosity. The micropores have molecular dimensions, the effective radii being less than 2 nm. The adsorption in these pores occurs through volume filling, and there is no capillary condensation taking place. They usually constitute the 95% of the total surface area of the activated carbon (1000–1500 $m^2$/g), being micropore volumes from 0.15 to 0.7 $cm^3$/g.

The activated carbons have surface area and pore volume that range between 250–2410 $m^2$/g and 0.022–91.4 $cm^3$/g, respectively [35]. Although the major part

of the adsorption take place through micro pores, the mesopores and macropores are also important due to enable sorbent molecules passing rapidly to smaller pores situated more internally.

Adsorption isotherms are usually experimentally determined in physical adsorption. The shape of an adsorption isotherm can provide preliminary qualitative information on the adsorption mechanism as well as on the porous structure of the carbons [36, 37 and 38]. The amount of gas adsorbed at a given temperature for different relative gas pressures is known as adsorption isotherms (IUPAC recognize 6 types of isotherms of physical adsorption [39]).

Numerous research works can be found in the literature concerning the estimation of properties related to the adsorption capacity of the activated carbons, i.e. specific surface, total volume of pores, pore size distribution, initial concentration of sorbent, temperature, degree of carbonization [40], contact time [24] and pH on the adsorption process [41, 42]. The effect of the temperature on the development of the porosity of a coal depends on the source material, heating rate and the residence time in the oven. The temperatures, where generally are reached good results in the pyrolysis and later on in the activation with $CO_2$ of lignocellulosic materials, are in the range between 350 °C and 850 °C [13, 23 and 43]. Out of these limits usually is not observed a significant improvement of the porosity.

A challenge in the production of activated carbon is to obtain very specific carbons with a given pore size distribution, from low cost materials [44] at low temperature. In this work, the preparation of activated carbon from a carbonaceous residue generated in a flash pyrolysis process of forestry waste (eucalyptus sp.) has been investigated.

The thermal degradation of a lignocellulosic material through a process of pyrolysis flash, for a short time and a high rate of heating, is commonly used for obtaining bio-oil [45, 46 and 47]. In contrast with other research works that have used eucalyptus wood as precursor material [12, 13], in this research is used a residue from a pyrolysis flash in order to valorize it. This residue was subjected to carbonization followed by carbon dioxide activation, in order to study the evolution of the specific surface and the porosity in relation to the activation temperature and the time of treatment.

## 2. Experimental

The main aspects that influence the activation of carbons are: the nature of the specimen, particle size, temperature, heating rate and residence time, in addition to the type of furnace and the process followed [48].

## 2.1. Raw material

The residue that has been investigated in this research is the product resulting from the flash pyrolysis of eucalyptus (barks, leaves and branches) at 650 °C in a fluidized bed reactor, vertical up-flow, at low pressure, and in the presence of a non-oxidizing atmosphere, sand bed and with recirculation of gases. Table 1 shows the main chemical features of this product. In the selection of the type of residue for the preparation of activated carbon, factors such as high carbon content, low inorganic compounds (i.e. low ash) content, or sufficient volatile matter content were taken into account [49].

By means of laser diffraction of the residue and the ashes were identified a significant presence of quartz ($SiO_2$). Because of the high intensity signal emitted by $SiO_2$, the presence of other minerals could be hidden. Therefore, it was carried out a demineralization with hydrochloric acid (HCl) to eliminated oxides, and later it was attacked with hydrofluoric acid (HF) to eliminate silicates. The resultant diffraction of the attacked product did not showed any peak. This could mean that the forestry waste was composed basically of organic matter, being the unique mineral substance presented the $SiO_2$, probably obtained when the lignocellulosic residues from pruning were collected.

## 2.2. Test set-up

Carbonization and activation tests of the residue have been carried out in a horizontal tubular furnace shown in Fig. 1.

With the introduction of $N_2$ into the circuit an inert atmosphere is achieved. $N_2$ from a cylinder is introduced into the circuit at a rate of 15 l/h, regulating the amount of gas by a flow controller.

The specimen is placed into a quartz tube of 75 mm diameter closed at both ends in order to confine the activation gases.

**Table 1.** Chemical characterization raw material & carbonaceous residue.

| | Proximate analysis (%, dry basis) | | | Moisture (as received) | Total sulfur (% dry basis) |
|---|---|---|---|---|---|
| | Ashes | Volatile matter | Fixed carbon | | |
| Forest residue | 4.11 | 73.75 | 22.14 | 4.50 | 0.08 |
| | 3.25 | 24.90 | 71.85 | 4.70 | 0.06 |
| | Elemental analysis (%, dry-ash free basis) | | | | |
| Carbonaceous residue | C | H | N | S | O $^*$ |
| | 74.25 | 3.67 | 0.18 | 0.05 | 21.85 |

$^*$ By difference.
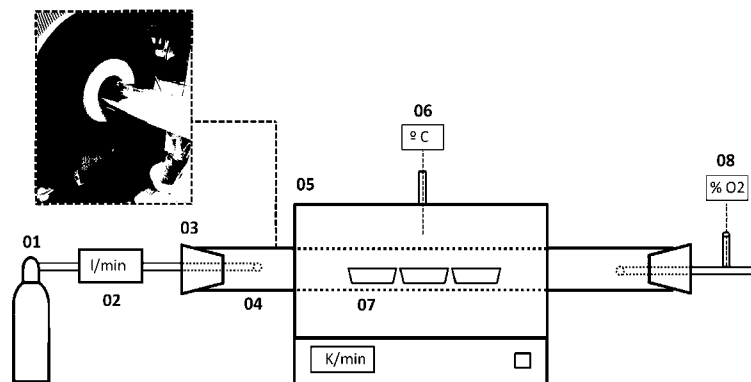
01: Gas cylinder ($N_2$/$CO_2$)

02: Mass flow controller

03: Silicone caps

04: Cylindrical quartz tube

05: Horizontal tubular furnace

06: Oven thermocouple

07: Ceramic vessels

08: Oxymeter

**Fig. 1.** Sketch of the experimental set and description of elements.

The programmable control of the oven allows, by means of a thermopar "Type K" situated in the centre of the tube, to establish the final heating temperature (electrically heated). It has been proved that the temperature gradient along the half-metre of the tube that is inside the oven is negligible. Therefore, in this part of the tube the temperature can be considered homogeneous.

The initial sample is placed in three ceramic vessels, and located in the central zone of the horizontal tube. By means of an oxygen detector is controlled the absence of this gas in the interior of the circuit.

Activation and carbonization processes are influenced by the heating rate and the decomposition temperature of biomass. Based on studies of other authors, where it has been observed that the heating rate vary between 5–20 K/min [50, 51, 52, 53 and 54], in this research it has been chosen a slow heating ramp of 7 K/min, where the development of secondary reactions are ensured (oil cracking and repolymerisation) [55] and it is allowed to obtain higher quantities of biochar.

The carbonization tests with $CO_2$ were carried out at different temperatures 400 °C, 600 °C and 800 °C, following research carried out from other authors [56, 57 and 58] using the same procedure. Each of the carbonized products obtained is activated to these same temperatures (i.e. the carbonized product at 400 °C was activated at 400 °C). The temperature of 400 °C was selected because is when the devolatilization of the three constituent polymers of lignocellulosic materials (hemicellulose, cellulose and lignin) is almost complete. In this research work an intermediate temperature of 600 °C was also selected, and then a maximum

temperature of 800 °C where the efficiency to obtain active carbon significantly decrease [59].

## 2.3. Carbonization

About 7.5 g of the sample (particle size <0.125 mm) was used in these experiments, which was carbonized under ultra-high purity nitrogen flow (250 ml. min$^{-1}$ STP). The preheating rate was 7 K/min to reach the carbonization temperatures (400 °C, 600 °C and 800 °C) maintaining these temperatures during 2 h, 4 h and 8 h.

## 2.4. Activation

In the following stage the physical activation was carried out with $CO_2$ at flow rate of 200 ml.min$^{-1}$STP. The activation temperatures were 400 °C, 600 °C and 800 °C with a heating rate of 7 K/min, and an activation time of 2 h, 4 h and 8 h. At the end of the activation process $N_2$ flow was again used during 2 h to reach the ambient temperature. The specimens of activated carbon were classified and preserved in a dryer to avoid the absorption of moisture from the ambient. Later on, the degree of porosity developed was analysed.

## 2.5. Characterization

Gas adsorption experiments were performed by using a Micromeritics ASAP 2000 analyzer, in order to determine the pore structure of both the chars and the activated carbons by $N_2$ adsorption-desorption at 77 K.

The surface area was determined by using the Brunauer, Emmett and Teller (BET) method, the micropore area and volume by using the Boer method and the total pore volume and pore size distribution by using the Barret-Joyner-Halenda (BJH) method.

Scanning electron micrographs (SEM) of selected samples were also obtained. The apparatus used was a Hitachi S-570 Scanning Electron Microscope to observe the presence of porosities and microporosities of the samples. The resolution was 3.5 nm, 20x-200.000x with an accelerating voltage between 0.5 and 30 kV. As the samples were not electrically conductive, they were gold plated (<10 nm) using a Polaron-Bio-Raid apparatus.

## 3. Results and discussion

### 3.1. Surface area and pore volume

Table 2 shows the results obtained during carbonization at three temperatures, needed for the characterization of the porous structure of the chars obtained. It is

**Table 2.** Characterization of the porous structure of biochar produced at different carbonization temperatures.

| Temp. (°C) | Time (h) | Ash (%) | Loss of weight (%) | Surface area BET (m²/g) | Micropore area (m²/g) | (%) | Total vol. BJH (cm³/g) | Micropore volume (cm³/g) | (%) | Average pore diameter (nm) |
|---|---|---|---|---|---|---|---|---|---|---|
| 400 | 2 | 3.9 | 8.90 | 52.13 | 4.82 | 9.25 | 0.0358 | 0.0017 | 4.71 | 2.749 |
|  | 4 | 4.2 | 8.98 | 37.52 | 4.08 | 10.87 | 0.0348 | 0.0013 | 3.80 | 3.711 |
| 600 | 2 | 4.4 | 23.11 | 370.49 | 296.39 | 80.00 | 0.1948 | 0.1381 | 70.14 | 1.594 |
|  | 4 | 4.0 | 23.97 | 367.25 | 298.97 | 81.41 | 0.1928 | 0.1389 | 72.03 | 1.576 |
| 800 | 2 | 4.8 | 30.53 | 435.09 | 366.69 | 85.02 | 0.2314 | 0.1728 | 74.68 | 1.582 |
|  | 4 | 5.4 | 29.92 | 436.51 | 371.10 | 77.38 | 0.2285 | 0.1736 | 75.95 | 1.571 |

shown that the temperature has a remarkable influence in the increase of the surface area BET and microporosity.

A change is observed in the transition from 400 °C to 600 °C, and also it continues increasing, to a lesser degree, at 800 °C; but on account of a high loss of matter (about 30%). However, there is not an influence of the time of treatment in the carbonization stage. Ash production remains practically constant in this period as it is shown in Table 2.

Table 3 reports the characterization of the porous structure of activated carbons prepared by using $CO_2$ flow at the same temperatures than the carbonization stage.

The maximum activation is achieved at the temperature of 800 °C, where there is a great influence of the activation time but, on the contrary, a high loss of matter (about 90%) is produced. Because of that, it was not considered to carry out the testing over 4 h.

At 600 °C there is a remarkable increase of the area and volume of micropores remaining practically invariant along this temperature, showing that the influence of time is not so significant. The figures of the BET surface area are influenced by the use of a precursor for the activated carbon. However, the activation process is less significant at 400 °C.

A difference among the activated samples is observed at 800 °C, where the time parameter increases the specific surface in a more pronounced manner than at 400 °C and 600 °C. Furthermore, in this temperature the greater increase of the specific area and volume of micro pores is produced. However, in comparison with the activated samples at 600 °C the micropores decrease at 800 °C, indicating that the material is mainly microporous at that temperature, and when is activated at higher temperature a development of mesoporosity is produced. This result is confirmed in the assessment of the figures obtained from average diameters, where at 600 °C the activated carbon presents the smallest pore diameter with the presence of plentiful micropores. When the activation temperature increases up to 800 °C the pore diameter grows in favour of the mesoporosity.

Gases removed during the thermal degradation of the lignocellulosic material are essentially $CO_2$, CO, $H_2$, $CH_4$, $C_2H_6$ and $C_2H_4$. These are significantly removed within the range of temperatures 305–375 °C [19]. So, it could be an explanation to the low sensitivity at higher temperatures (600 °C and 800 °C in this study) when activation occurs. This can be also observed in other studies [13], once it has been developed microporosity (as in the case of the eucalyptus in this study at 600 °C) the activation time also seems to have less influence.

**Table 3.** Characterization of the porous structure of activated carbon by $CO_2$ flow at different temperatures.

| Temp. | Time | Ash | Loss of weight | Surface area BET | Micropore area | | Total vol. BJH | Micropore volume | | Average pore diameter |
|---|---|---|---|---|---|---|---|---|---|---|
| (°C) | (h) | (%) | (%) | (m²/g) | (m²/g) | (%) | (cm³/g) | (cm³/g) | (%) | (nm) |
| 400 | 2 | 3.6 | 9.10 | 72.97 | 8.15 | 11.17 | 0.0391 | 0.0016 | 4.17 | 2.144 |
| | 4 | 3.5 | 10.11 | 134.56 | 17.76 | 13.20 | 0.0689 | 0.0038 | 5.59 | 2.048 |
| | 8 | 3.9 | 11.11 | 181.78 | 62.00 | 34.10 | 0.0933 | 0.0257 | 27.60 | 2.054 |
| 600 | 2 | 4.7 | 13.33 | 376.70 | 304.74 | 80.90 | 0.1948 | 0.1425 | 73.17 | 1.546 |
| | 4 | 5.0 | 25.03 | 389.96 | 336.69 | 86.34 | 0.1987 | 0.1563 | 78.66 | 1.539 |
| | 8 | 5.2 | 27.25 | 410.06 | 326.02 | 79.50 | 0.2186 | 0.1570 | 71.81 | 1.547 |
| 800 | 2 | 10.6 | 66.77 | 905.02 | 544.36 | 55.13 | 0.5488 | 0.2538 | 46.24 | 1.794 |
| | 4 | 25.4 | 89.88 | 1034.07 | 570.09 | 63.23 | 0.6129 | 0.2596 | 42.35 | 1.779 |

## 3.2. Pore size distribution

Fig. 2 shows the 77 K adsorption-desorption isotherms of activated carbons obtained at different temperatures by using $CO_2$. It is observed that at 400 °C and 600 °C the adsorption isotherms are typical of the microporous activated carbons, showing the phenomenon so-called low pressure hysteresis, due to the deformation of the micropores caused by the sorbent during the adsorption process. Assessing the volume of the micropores, it is checked that the microporosity is inside the rank of the narrow micropores, i.e. those micro pores filled at very low relative pressures as consequence of the high adsorption potential between their walls. In the series of 800 °C the isotherms of the activated samples showed hysteresis, characteristic of capillary condensation in the mesopores. This suggests that the activation at high temperature develops the mesoporosity, as it could be seen by the increase of the slope in the adsorption branch when the activation time increases. These types of hysteresis cycles seem to be associated to the narrow pores with the shape of "horseshoe", frequent in active carbons.

In order to provide further information, the sample was analysed performing SEM analysis. The sample was firstly carbonized and then activated with $CO_2$. Therefore, the internal porous structure of the material obtained could be observed.

## 3.3. Particle morphology characterization

In Fig. 3 are shown Scanning Electron Microscopy (SEM) micrographs of a carbonized sample 120x-1.200x at 800 °C during 4 h. In this figure it is observed the morphological structure, where disorganized narrow pores are found.
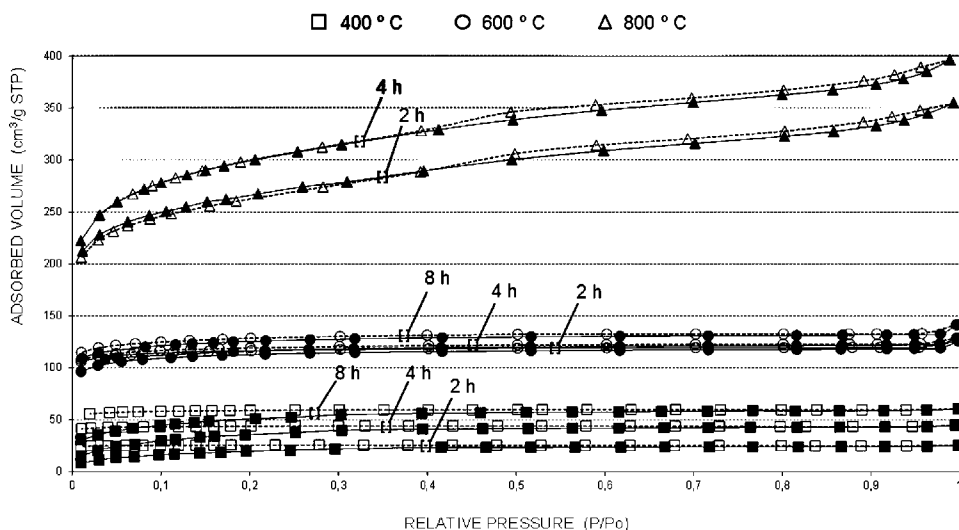


**Fig. 2.** 77 K N2 adsorption-desorption isotherms of active carbons obtained by $CO_2$ activation at different burned levels. (Continuous lines–adsorption and dashed lines–desorption).
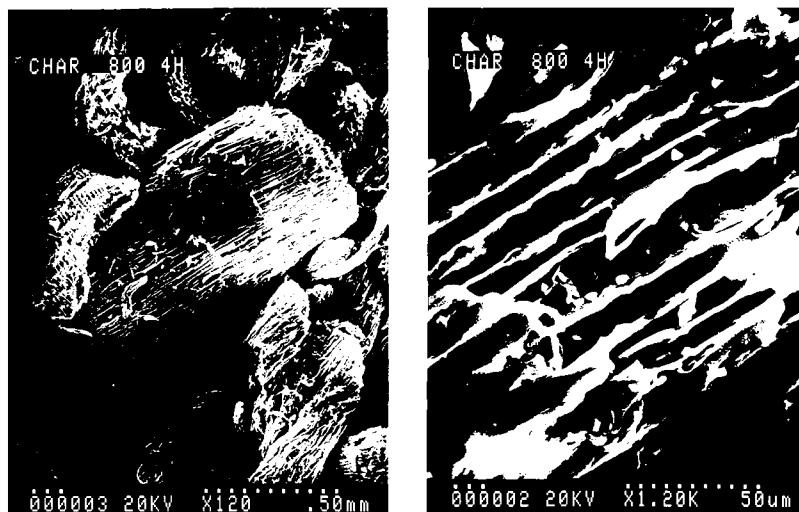
**Fig. 3.** SEM of a sample prepared by carbonization at 800 °C during 4 h.

As a consequence of the carbonization, changes were produced in the original structure of the sample of eucalyptus. In this way, it was obtained a solid and homogeneous material with presence of abundant grooves. A grooved structure of carbon is observed in the surface that folds up because of the temperature, as well as the presence of loose material that must be eliminated through sweep activation gas in the later stage.

In Fig. 4 are shown SEM micrographs of an activated sample, at 800 °C during 4 h. In these figures narrow pores appeared with a characteristic "horseshoe" shape being consistent the results shown in Fig. 2.



**Fig. 4.** SEM of a sample activated at 800 °C during 4 h.

In the activation stage the superficial morphology of the material change to cylindrical with the presence of abundant pores connected that allows the access to the micro porous internal zones. The carbonaceous structure that is obtained is much weaker as a consequence of the material loss.

## 4. Conclusions

The carbonization stage of the carbonaceous residue generated in a flash pyrolysis process of eucalyptus devolatilises the char and creates a microporous structure which falls mainly within the rank of narrow micropores.

The maximum physical activation with $CO_2$ flow has been produced at 800 °C with a well-developed porosity compatible with BET apparent surface area values, similar to those of commercial activated carbons used as adsorbents in gas and liquid-phase separation processes, purification of products and gas and water cleaning operations. At this temperature there is great influence of the time parameter of activation, but on the contrary a high loss of matter is produced (about 90%).

Although the activation at 600 °C is higher than at 400 °C, in both of them the influence of the time is not significant, remaining practically constant.

The activated carbon obtained shows the lowest pore diameter at 600 °C, and when the activation temperature increases up to 800 °C the pore diameter grows in favour of the mesoporosity.

The $N_2$ adsorption-desorption isotherms forms of the active carbon obtained by $CO_2$ activation indicate the form and size of the pores. Those verify at 800 °C the presence of mesoporosity, while at 400 °C and 600 °C the isotherms are typical of microporosity carbons, with low pressure hysteresis phenomenon.

The temperature reached during the pyrolization and activation processes is responsible of the internal folding of the carbonaceous structure, obtaining morphology of the residue organized in cylindrical layers.

## 5. Declarations

### Author contribution statement

Carlos Grima-Olmedo: Conceived and designed the experiments; Performed the experiments; Analyzed and interpreted the data; Contributed reagents, materials, analysis tools or data; Wrote the paper.

Álvaro Ramírez-Gómez: Conceived and designed the experiments; Performed the experiments; Analyzed and interpreted the data; Wrote the paper.

Dulce Gómez-Limón: Performed the experiments; Analyzed and interpreted the data.

Carmen Clemente-Jul: Analyzed and interpreted the data; Contributed reagents, materials, analysis tools or data.

## Funding statement

## Competing interest statement

The authors declare no conflict of interest.

## Additional information

No additional information is available for this paper.

## References

[1] O.S. Amuda, A.A. Giwa, I.A. Bello, Removal of heavy metal from industrial wastewater using modified activated coconut shell carbon, Biochem. Eng. J. 36 (2) (2007) 174–181.

[2] M.F. Alkhatib, S.A. Muyibi, J.O. Amode, Optimization of activated carbon production from empty fruit bunch fibers in one-step steam pyrolysis for cadmium removal from aqueous solution, Environmentalist 31 (2011) 349–357.

[3] S.M. Mosa, Adsorption of some heavy metals and (Mg2+, Ca2 +) ions from aqueous solutions by using different environmental residuals as a cheap adsorbents at optimum conditions, Sci. J. Chem. 2 (1) (2014) 1–5.

[4] S. Babel, T.A. Kurniawan, Cr(VI) removal from synthetic wastewater using coconut shell charcoal and commercial activated carbon modified with oxidizing agents and/or chitosan, Chemosphere 54 (7) (2004) 951–967.

[5] M. Dabioch, R. Skorek, A. Kita, P. Janoska, K. Pytlakowsha, P. Zerzucha, R. Sitko, A study on adsorption of metals by activated carbon in a large-scale (municipal) process of surface water purification, Cent. Eur. J. Chem. 11 (5) (2013) 742–753.

[6] S. Altenor, B. Carene-Melane, S. Gaspard, Activated carbons from lignocellulosic waste materials for water treatment: a review, International Journal of Environmental Technology and Management 10 (3/4) (2009) 308–326.

[7] J. Reungoat, B.I. Escher, M. Macova, F.X. Argaud, W. Gernjak, J. Keller, Ozonation and biological activated carbon filtration of wastewater treatment plant effluents, Water Res. 46 (2012) 863–872.

[8] M. Boehler, B. Zwickenpflug, J. Hollender, T. Ternes, A. Joss, H. Siegrist, Removal of micropollutants in municipal wastewater treatment plants by powder-activated carbon, Water Sci. Technol. 66 (10) (2012) 2115–2121.

[9] M.A. Sidheswaran, H. Destaillats, D.P. Sullivan, S. Cohn, W.J. Fisk, Energy efficient indoor VOC air cleaning with activated carbon fiber (ACF) filters, Build Environ. 47 (2012) 357–367.

[10] H.F.L. Wertheim, D.M. Ngoc, M. Wolbers, T.T. Binh, N. Thi, T. Hai, et al., Studying the effectiveness of activated carbon R95 respirators in reducing the inhalation of combustion by-products in Hanoi, Vietnam: a demonstration study, Environ. Health 11 (72) (2012).

[11] A. Hironobu, Hysteresis in water vapor adsorption and desorption isotherms of activated carbon products used in Japanese gas respirators, Sangyo eiseigaku zasshi = Journal of occupational health 52 (5) (2010) 216–218.

[12] N. Tancredi, T. Cordero, J. Rodriguez Mirasol, J.J. Rodriguez, Activated carbons from uruguayan eucalyptus wood, Fuel 75 (15) (1996) 1701–1706.

[13] Y. Ngernyen, C. Tangsathitkulchai, M. Tangsathitkulchai, Porous properties of activated carbon produced from eucalyptus and Wattle wood by carbon dioxide, Korean J. Chem. Eng. 23 (6) (2006) 1046–1054.

[14] M. Kumar, R.C. Gupta, Influence of carbonization conditions on the gasification of acacia and eucalyptus wood chars by carbon-dioxide, Fuel 73 (12) (1994) 1922–1925.

[15] M. Yoshinaga, Production of char using waste wood and its application to the removal of pollutants in flue gases, Eurocarbon. Berlin II (2000) 643.

[16] Kazehaya A Hayashi, K. Muroyama, A.P. Watkinson, Preparing an activated carbon from lignin by chemical activation with $K_2CO_3$, Eurocarbon. Berlin II (2000) 585.

[17] M.M. Mourao, P.J.M. Carrott, M.M.L. Ribeiro, Preparation of activated carbons from cork oak, Eurocarbon. Berlin II (2000) 639.

[18] K. Gergova, S. Eser, Effects of activation method on pore structure of activated carbons from apricot stones, Carbon 34 (7) (1996) 879–888.

[19] R. Malik, D.S. Ramteke, S.R. Wate, Physico-chemical and surface characterization of adsorbent prepared from groundnut shell by ZnCl2

activation and its ability to adsorb colour, Indian J. Chem. Technol. 13 (4) (2006) 319–328.

[20] S. Somasundaram, K. Sekar, V.K. Gupta, S. Ganesan, Synthesis and characterization of mesoporous activated carbon from rice husk for adsorption of glycine from alcohol-aqueous mixture, J. Mol. Liq. 177 (2013) 416–425.

[21] A.N.A. El-Hendawy, Surface and adsorptive properties of carbons prepared from biomass, Appl. Surf. Sci. 252 (2) (2005) 287–295.

[22] J. Alcañiz-Monge, C. Blanco, A. Linares-Solano, R. Brydson, B. Rand, Development of new carbon honeycomb structures from cellulose and pitch, Eurocarbon. Berlin II (2000) 483.

[23] L.M. Cotoruelo, M.D. Marques, F.J. Diaz, J. Rodriguez-Mirasol, J.J. Rodriguez, T. Cordero, Adsorbent ability of lignin-based activated carbons for the removal of p-nitrophenol from aqueous solutions, Chem. Eng. J. 184 (2012) 176–183.

[24] A. Jain, S.K. Tripathi, Converting eucalyptus leaves into mesoporous carbon for its application in quasi solid-state supercapacitors, J. Solid State Electr. 17 (9) (2013) 2545–2550.

[25] P. Patnukao, P. Pavasant, Activated carbon from eucalyptus camaldulensis-dehnbark using phosphoric acid activation, Bioresource Technol. 99 (17) (2008) 8540–8543.

[26] A. Heidari, H. Younesi, A. Rashidi, A. Ghoreyshi, Adsorptive removal of $CO_2$ on highly microporous activated carbons prepared from eucalyptus camaldulensis wood: Effect of chemical activation, J. Taiwan Inst. Chem. E. 45 (2) (2014) 579–588.

[27] R. Wang, Y. Amano, M. Machida, Surface properties and water vapor adsorption-desorption characteristics of bamboo-based activated carbon, J. Anal. Appl. Pyrol. 104 (2013) 667–674.

[28] Dokuritsu Gyosei Hojin Sangyo Gijutsu So. Osu kk, Manufacture of carbonized material such as activated carbon/decomposition product such as hydrogen gas, involves introducing raw material and water vapor into furnace and carbonizing raw material by supplying superheated steam, (2016) Patent Number: JP2008063169-A; JP5282323-B2.

[29] T. Budinova, K. Gergova, N. Petrov, V. Minkova, A study of the process of pyrolysis in a water-vapor stream of activated carbons, prepared from agricultural by-products by some physicochemical methods, Thermochimica Acta 244 (1994) 267–276.

[30] K. Gergova, A. Galushko, N. Petrov, V. Minkova, Investigation of the porous structure of activated carbons prepared by pyrolysis of agricultural by-products in a stream of water-vapor, Carbon 30 (5) (1992) 721–727.

[31] M. Beatriz Vazquez-Santos, A. Martinez-Alonso, J.M.D. Tascon, Effects of phosphoric acid as additive in the preparation of activated carbon fibers from poly (p-phenylene benzobisoxazole) by carbon dioxide activation, J. Anal. Appl. Pyrol. 95 (2012) 68–74.

[32] J. Alcaniz-Monge, M. Perez-Cadenas, J.P. Marco-Lozar, Removal of harmful volatile organic compounds on activated carbon fibres prepared by steam or carbon dioxide activation, Adsorpt. Sci. Technol. 30 (6) (2012) 473–482.

[33] V. Sricharoenchaikul, C. Pechyen, D. Aht-ong, D. Atong, Preparation and characterization of activated carbon from the pyrolysis of physic nut (jatrophacurcas L.) waste, Energy Fuels. 22 (1) (2008) 31–37.

[34] A. Ahmadpour, D.D. Do, The preparation of activated carbon from macadamia nutshell by chemical activation, Carbon 35 (12) (1997) 1723–1732.

[35] O. Ioannidou, A. Zabaniotou, Agricultural residues as precursors for activated carbon production-A review, Renew. Sust. Energ. Rev. 11 (2007) 1966–2005.

[36] L. Khezami, A. Chetouani, B. Taouk, R. Capart, Production and characterisation of activated carbon from wood components in powder: Cellulose, lignin, xylan, Powder Technol. 157 (1–3) (2005) 48–56.

[37] R. Arriagada, R. Garcia, M. MolinaSabio, F. RodriguezReinoso, Effect of steam activation on the porosity and chemical nature of activated carbons from Eucalyptus globulus and peach stones, Microporous Mater. 8 (3–4) (1997) 123–130.

[38] N. Tancredi, N. Medero, F. Moller, J. Piriz, C. Plada, et al., Phenol adsorption onto powdered and granular activated carbon, prepared from Eucalyptus wood, J. Colloid Interf. Sci. 279 (2) (2004) 357–363.

[39] K.S.W. Sing, D.H. Everett, R.A.W. Haul, L. Moscou, R.A. Pierotti, J. Rouquerol, et al., Pure Appl. Chem. 57 (1985) 603.

[40] J. Rodriguez-Mirasol, T. Cordero, J.J. Rodriguez, Preparation and characterization of activated carbons from eucalyptus kraft lignin, Carbon 31 (1) (1993) 87–95.

[41] J.M.V. Nabais, J.A. Gomes, P.J.M. Suhas Carrott, C. Laginhas, S. Roman, Phenol removal onto novel activated carbons made from lignocellulosic

precursors: Influence of surface properties, J. Hazard Mater. 167 (1–3) (2009) 904–910.

[42] P. Patnukao, A. Kongsuwan, P. Pavasant, Batch studies of adsorption of copper and lead on activated carbon from Eucalyptus camaldulensis Dehn. Bark, J. Environ. Sci-China 20 (9) (2008) 1028–1034.

[43] S.G. Herawan, M.S. Hadi, R. Ayob Md, A. Putra, Characterization of Activated Carbons from Oil-Palm Shell by CO2 Activation with No Holding Carbonization Temperature, The Scientific World Journal (2013) 1–6.

[44] M. Konstantinou, I. Pashalidis, Competitive sorption of Cu(II) and Eu(III) ions on olive-cake carbon in aqueous solutions-a potentiometric study, Adsorption 16 (3) (2010) 167–171.

[45] M. Amutio, G. Lopez, R. Aguado, J. Bilbao, M. Olazar, Biomass oxidative flash pyrolysis: autothermal operation, yields and product properties, Energy Fuels 26 (2012) 1353–1362.

[46] M.I. Jahirul, M.G. Rasul, A.A. Chowdhury, N. Ashwath, Biofuels production through biomass pyrolysis −a technological review, Energies 5 (2012) 4952–5001.

[47] A.V. Bridgwater, D. Meier, D. Radlein, An overview of fast pyrolysis of biomass, Org. Geochem. 30 (1999) 1479–1493.

[48] Tao Kan, Vladimir Strezov, Tim J. Evans, Evans Lignocellulosic biomass pyrolysis: A review of product properties and effects of pyrolysis parameters, Renewable and Sustainable Energy Reviews 57 (2016) 1126–1140.

[49] S.L. Rincon, A. Gomez, Comparative behaviour of agricultural biomass residues during thermochemical processing, Global Nest J. 14 (2) (2012) 111–117.

[50] P.T. Williams, S. Besler, The influence of temperature and heating rate on the pyrolysis of biomass, Renew. Energy 7 (1996) 233–250.

[51] Song-Yung Wang, Ming-Hsiu Tsai, Sheng-Fong Lo, Ming-Jer Tsai, Effects of manufacturing conditions on the adsorption capacity of heavy metal ions by Makino bamboo charcoal, Bioresour. Technol. 99 (2008) 7027–7033.

[52] Sait Yorgun, Naile Vural, Hakan Demiral, Preparation of high-surface area activated carbons from Paulownia Wood by ZnCl2 activation, Micropor. Mesopor. Mat. 122 (2009) 189–194.

[53] M.A. Naeem, M. Khalid, M. Arshad, R. Ahmad, Yield and nutrient composition of biochar produced from different feedstocks at varying pyrolytic tempera-tures, Pak. J. Agr. Sci. 51 (2014) 75–82.

[54] A. Abdel-Nasser El-Hendawy, S.E. Samra, B.S. Girgis, Adsorption characteristics of activated carbons obtained from corncobs, Colloids and Surfaces A: Physicochemical and Engineering Aspects 180 (3) (2001) 209–221.

[55] J.E. White, W.J. Catallo, B.L. Legendre, Biomass pyrolysis kinetics: a comparative critical review with relevant agricultural residue case studies, J. Anal. Appl. Pyrol. 91 (2011) 1–33.

[56] K. Sun, J. Jiang, Preparation and characterization of activated carbon from rubber-seed shell by physical activation with steam, Biomass and bioenergy 34 (2010) 539–544.

[57] A. Aworn, P. Thiravetyan, W. Nakbanpote, Preparation and characteristics of agricultural waste activated carbon by physical activation having micro- and mesopores, J. Anal. Appl. Pyrolysis 82 (2008) 279–285.

[58] C. Bouchelta, M.S. Medjram, O. Bertrand, J.P. Bellat, Preparation and characterization of activated carbon from date stones by physical activation with steam, J. Anal. Appl. Pyrolysis 82 (2008) 70–77.

[59] Yuvarat Ngernyen, Chaiyot Tangsathitkulchai, Malee Tangsathitkulchai, Porous properties of activated carbon produced from Eucalyptus and Wattle wood by carbon dioxide activation, Korean J. Chem. Eng. 23 (6) (2006) 1046–1054.